

Defect formation in *a*-Si:H

K. Winer*

Xerox Corporation, Palo Alto Research Center, Palo Alto, California 94304

(Received 16 January 1990)

The bulk chemical processes responsible for defect equilibria in hydrogenated amorphous silicon (*a*-Si:H) are examined. Thermodynamic analyses of the corresponding chemical reactions are shown to account quantitatively for the observed defect-state-energy distribution and dependence of the defect concentration on temperature and Fermi energy. The dependence of *a*-Si:H defect properties on growth conditions is addressed.

I. INTRODUCTION

At the absolute zero of temperature, single-crystalline semiconductors like silicon (*c*-Si) are in their thermodynamic ground states; because the entropy component is zero, the minimum-free-energy condition can only be satisfied by the absence of defects. As the temperature is raised, lattice defects form whose concentrations depend exponentially on inverse temperature. The kinetics of defect equilibration is limited by the rate of lattice atom or defect diffusion, and nonequilibrium concentrations of defects can be "frozen in" if the thermal quench rate is faster than the equilibration rate at the quench temperature. The equilibrium between a lattice and its defects can be simply described by one or more chemical reactions, and the solid-state chemistry of defects in crystals is a well-developed science.¹

Amorphous semiconductors, in contrast, are always far from the thermodynamic ground state of their crystalline counterparts. The nonequilibrium nature of their growth and structure was long thought to preclude the solid-state chemistry that occurs in all crystalline materials. Therefore, it was surprising when both the active-dopant² and deep-defect³ concentrations in hydrogenated amorphous silicon (*a*-Si:H) were recently discovered to depend in a reversible manner on temperature. From this discovery, a new and powerful framework for understanding *a*-Si:H material properties has emerged that describes the processes of defect formation and dopant activation by simple chemical reactions whose kinetics are determined by dispersive hydrogen diffusion.⁴ This chemical description permits accurate, quantitative theories of *a*-Si:H behavior to be constructed that depend on only a few experimentally measurable parameters. The importance of such a capability cannot be overstated for a material whose short-range structural and compositional disorder, lack of translational symmetry, and varied microstructure preclude the use of the Bloch theorem to describe its properties.

The analysis of chemical reactions in *a*-Si:H borrows heavily from the methods developed to analyze defect reactions in crystals, but the disordered nature of *a*-Si:H introduces distributions of reaction enthalpies and diffusion barriers that result in several novel effects not found in

crystals. Also, while the kinetics of vacancy formation in *c*-Si depends on Si motion, which occurs appreciably only at high ($\sim 1000^\circ\text{C}$) temperatures, it is the dispersive diffusion of hydrogen that mediates the solid-state chemical reactions in *a*-Si:H, governs their kinetics, and allows equilibrium to be achieved at relatively low ($\sim 200^\circ\text{C}$) temperatures. This is not a global equilibrium in which all network constituents that contribute to the electronic structure of the material participate. Instead, it is the equilibrium between small subsets of localized states that determines the defect and dopant concentrations in *a*-Si:H.

In the following we develop a quantitative theory of defect formation in *a*-Si:H based on the thermodynamic analysis of a few simple chemical reactions. Analytical expressions for the equilibrium defect concentrations and defect-state-energy distributions in *a*-Si:H are derived as a function of temperature and Fermi energy and compared with the available experimental data. The dependence of *a*-Si:H defect properties on growth conditions is addressed.

II. THERMODYNAMICS OF *a*-Si:H: THERMAL, MECHANICAL, AND CHEMICAL EQUILIBRIUM

When the active-dopant and neutral-defect concentrations in *a*-Si:H were first discovered to vary reversibly with temperature, the effect was thought to be strictly thermal and was hence referred to as thermal equilibration.^{2,3} While the active-dopant and neutral-defect concentrations do indeed depend on temperature, the long equilibration times (up to one year at 300 K in *n*-type *a*-Si:H) make it clear that some other type of equilibrium is involved.

Consider the differential of the Gibbs free energy (thermodynamic potential)⁵

$$dG = -S dT + V dP + \sum_i \mu_i dn_i, \quad (1)$$

where S is entropy, T is temperature, P is pressure, V is volume, and μ_i and n_i are the chemical potential and number of moles, respectively, of chemical species i . At thermodynamic equilibrium $dG \equiv 0$ and the temperature,

pressure, and number of moles of each species is constant. If we imagine an experiment where a sample of *a*-Si:H, initially at equilibrium at a temperature T , is placed in contact with a heat reservoir at temperature T^* , we should expect that within a few phonon cycle times (~ 100 ps) thermal equilibrium will be achieved so that the sample temperature is everywhere T^* . The first term in Eq. (1) will then be zero. Once the phonons in the sample equilibrate with those in the heat reservoir and a temperature can be defined, the volume of the sample will be fixed. As long as no work is being done on or by the sample, it will be in mechanical equilibrium and the second term in Eq. (1) will be zero. The third term in Eq. (1) will vary as the concentration of each species changes during the approach to thermodynamic equilibrium. These concentration changes occur due to the conversion of one species into another, in a manner specified by chemical reactions and at rates determined by the rates of species motion. In general, these rates are small so that the thermodynamic equilibration ($dG \rightarrow 0$) will be limited by the rate of chemical equilibration ($\sum_i dn_i \rightarrow 0$) amongst the chemical species in the system.

Thus, the distinction between thermal and chemical equilibrium is not merely a semantic one. Thermal equilibrium occurs when the rates of heat exchange between a system and its surroundings are equal. Thermal equilibration is generally mediated by phonon (or photon) transport. Chemical equilibrium occurs when the forward and reverse rates of a chemical reaction are equal. Chemical equilibration is generally mediated by atomic (or molecular) transport. This distinction is important because chemical reactions, not phonon exchange processes, are the key to interpreting the behavior of defects in *a*-Si:H.

Consider a chemical reaction between two species A and B (i.e., $A \rightleftharpoons B$) characterized by states a and b , whose energy difference is $\Delta E = E_b - E_a$ and which are separated by an energy barrier E' . At equilibrium, the concentration of B according to the law of mass action is given by⁵

$$[B]_{\text{eq}} = [A]_{\text{eq}} \exp(-\Delta E/kT). \quad (2)$$

When the system equilibrium is perturbed, simple reaction-rate theory predicts that the concentration of B will equilibrate exponentially fast, i.e.,

$$[B](t) - [B]_{\text{eq}} = \{[B](0) - [B]_{\text{eq}}\} \exp(-t/\tau), \quad (3)$$

where the equilibration time constant $\tau = \tau_0 \exp[(E' - E_b)/kT]$. These relations are well established for defect reactions in crystals. However, the disordered nature of *a*-Si:H introduces distributions of reaction enthalpies ΔE and energy barriers E' , which require significant modifications of the above relations. The modification of the kinetic equation (3) has been treated by Jackson.⁶ The modification of the equilibrium equation (2) is treated below.

III. INGREDIENTS OF A THEORY OF DEFECT FORMATION

In optimally grown undoped *a*-Si:H, the neutral-defect concentration $[D^0]$ frozen in at growth (230°C) is typi-

cally 10^{16} cm^{-3} or less.³ If a simple two-state equilibrium such as $\text{Si} \rightleftharpoons D^0$ were responsible for this defect concentration, we should expect that, like Eq. (2),

$$[D^0]_{\text{eq}} = [\text{Si}]_{\text{eq}} \exp(-\Delta E/kT), \quad (4)$$

where $[\text{Si}]_{\text{eq}} \approx 5 \times 10^{22} \text{ cm}^{-3}$ is the concentration of Si atoms in *a*-Si:H. This would require $\Delta E \approx 0.7 \text{ eV}$ for $[D^0] = 10^{16} \text{ cm}^{-3}$ so that $[D^0]$ should be highly temperature dependent. In fact, ΔE has been measured to be between 0.2 and 0.3 eV;^{3,7-9} the equilibrium must be between neutral defects and a much smaller subset of the network constituents, whose concentration lies between 10^{18} and 10^{19} cm^{-3} . Other than Si or H ($[\text{H}] \approx 5 \times 10^{21} \text{ cm}^{-3}$), it is not obvious what other intrinsic chemical species might correspond to this small subset.

A. Weak-bond–dangling-bond conversion

Smith and Wagner¹⁰ resolved this difficulty by invoking the weak-bond–dangling-bond conversion model originally proposed by Stutzmann¹¹ to account for the increase of the defect concentration upon doping in *a*-Si:H. Stutzmann's idea was that as the Fermi energy moved into the localized band-tail states (weak-bond states) with doping, electrons (*n*-type) or holes (*p*-type) would occupy antibonding levels of these states and make bond breaking, and hence defect formation, easier. Smith and Wagner treated this weak-bond–dangling-bond conversion as a chemical reaction and applied the result to calculate the neutral-defect concentration at equilibrium in undoped *a*-Si:H. It is clear that this procedure will resolve the numerical difficulty encountered in Eq. (4), since the concentration of weak bonds in *a*-Si:H is $\approx 10^{19} \text{ cm}^{-3}$, just what is required by the simple theory.

The original analysis was performed by minimizing an expression for the free energy of the weak-bond–dangling-bond ensemble, similar to the analysis of Schottky defect formation.¹⁰ An equivalent procedure is to apply the law of mass action to the proposed weak-bond–dangling-bond reaction



where SiSi are weak Si–Si bonds and D^0 are neutral defects. At equilibrium,

$$[D^0]_{\text{eq}} = [\text{SiSi}]_{\text{eq}} \exp(-\Delta E/kT), \quad (6)$$

by the law of mass action, and

$$\begin{aligned} [\text{SiSi}]_{\text{tot}} &= [\text{SiSi}]_{\text{eq}} + [\text{SiSi}]_{\text{broken}} \\ &= [\text{SiSi}]_{\text{eq}} + [D^0]_{\text{eq}}, \end{aligned} \quad (7)$$

by the conservation of bonds, since each broken bond produces one defect by construction; $[\text{SiSi}]_{\text{tot}}$ is the total concentration of weak bonds in the absence of defects. Therefore,

$$[D^0]_{\text{eq}} = \frac{[\text{SiSi}]_{\text{tot}}}{1 + \exp(\Delta E/kT)}. \quad (8)$$

The most important contribution made by Smith and Wagner is their recognition that the weak-

bond–dangling-bond reaction is not characterized by a single-reaction enthalpy ΔE , but rather by a distribution of reaction enthalpies determined by the slope of the valence-band tail.¹⁰

B. Distribution of reaction enthalpies

The existence of a distribution of reaction enthalpies is made clear in Fig. 1, which depicts the valence-band tail (weak SiSi bonding states) described by $N_{v0}\exp(-E/E_0)$, where N_{v0} is the peak density of states and E_0 is the slope of the valence-band tail, and a single defect (D^0) state in the gap at E_{D^0} . The concentration of weak-bond states in the interval between E and $E+dE$ is $\rho_{\text{SiSi}}(E) = N_{v0}\exp(-E/E_0)dE$, exactly twice the concentration of weak bonds [SiSi] whose states lie in this energy interval. The enthalpy for reaction (5) is the cost to remove a weak-bonding state at E and create a defect state at E_{D^0} . This energy cost can be taken to be equal to the one-electron energy difference between the weak-bonding states at E and the defect state at E_{D^0} when ionic relaxation and multielectronic effects are ignored.¹⁰

This approximation for defect-formation energies was first proposed for α -Si:H by Stutzmann in connection with the weak-bond–dangling-bond conversion model.¹¹ However, as discussed by Heine,¹² this approximation is generally valid to describe defect-formation energies in solids because either the ionic relaxation and multielectronic contributions to the formation energies are small or they cancel each other out. It seems reasonable that, because α -Si:H is already highly disordered, relaxation energies should be small in this material. The validity of this approximation has yet to be tested in α -Si:H by detailed calculation, although its use in the analysis of defect-formation reactions seems to provide excellent agreement with the experimental data. This approximation implies a mapping between defect sites and states on the one

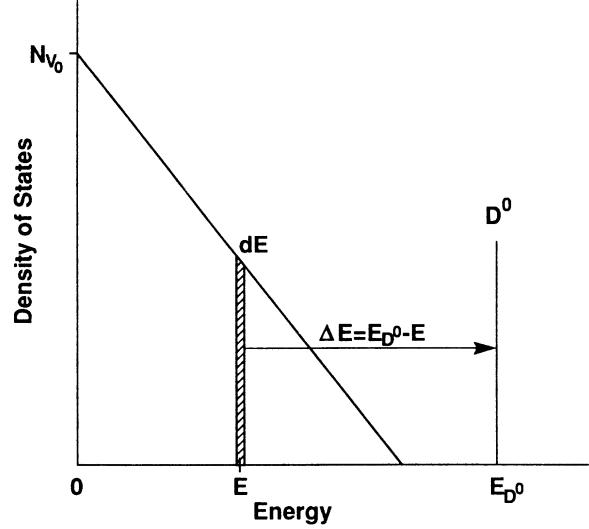


FIG. 1. Schematic density-of-states diagram to illustrate the distribution of reaction enthalpies in the weak-bond–dangling-bond conversion model of Schottky defect formation according to reaction (5). The reaction enthalpy is the cost to convert a weak-bond state at E into a defect state at E_{D^0} ; the one-electron energy difference $\Delta E = E_{D^0} - E$. All weak-bond states from $E = 0$ to $E \rightarrow \infty$ contribute to the reaction.

hand, and weak-bond sites and states on the other, which allows the species and their electronic states to be treated interchangeably.

Taking the enthalpy for reaction (5) to be $\Delta E = E - E_{D^0}$, the total concentration of defects whose states lie at energy E_{D^0} is given by integrating Eq. (8) over the integration variable E from E_{v0} ($\equiv 0$) to infinity to obtain

$$\begin{aligned}
 [D^0]_{\text{eq}} &= \frac{1}{2} \int_0^{\infty} \frac{N_{v0}\exp(-E/E_0)}{1 + \exp[(E - E_{D^0})/kT]} dE \\
 &= \frac{1}{2} \left[\frac{N_{v0}E_0kT}{(E_0 - kT)} \right] \left[\frac{E_0}{kT} \exp(-E_{D^0}/E_0) - \exp(-E_{D^0}/kT) \right]. \quad (9)
 \end{aligned}$$

The analysis results in a simple, formal expression for the neutral-defect concentration at equilibrium as a function of a few experimentally measurable parameters. It is clear from Eq. (9) that the ratio of sample temperature T and effective valence-band-tail temperature T_v ($\equiv E_0/k$) is a crucial determinant of the defect concentration of α -Si:H. As long as T is near or below $T_v \approx 520$ K, the temperature dependence of $[D^0]$ will be weak, as is observed. Also, the experimental correlation between defect concentration and Urbach energy (closely related to E_0) is explicit in Eq. (9).^{13,14} These features are a great success of the weak-bond–dangling-bond conversion model and its analysis as a chemical reaction. However, there is a

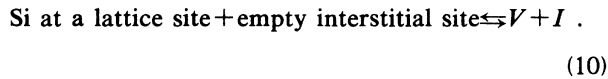
problem with reaction (5).

The problem is that one broken bond should lead to two rather than one defect. Smith and Wagner modified their analysis to take this extra defect into account,¹⁵ but a more serious problem remains. In order for a broken weak bond to be spin active, the two resulting dangling-bond defects must diffuse away from each other. The problem with the reaction $\text{SiSi} \rightleftharpoons 2D^0$ is that there is no mechanism by which the two resulting dangling bonds can accomplish this. Such a mechanism is likely to determine the reaction kinetics. The kinetics of defect equilibration in α -Si:H has been measured and is consistent with a process whose rate is limited by the dispersive

diffusion of hydrogen.^{4,9,16–18} The explicit introduction of H into the chemical reactions describing defect formation resolves the problem of defect diffusion and accounts for the kinetics of defect equilibration in a straightforward manner.

C. Hydrogen-mediated defect reactions

Smith and Wagner modeled defect creation in *a*-Si:H on Schottky defect formation in crystals. With the introduction of H into the defect reaction, the more appropriate crystalline model is Frenkel defect formation. In *c*-Si, Frenkel defects (Si vacancies V and interstitials I) are generated according to the reaction

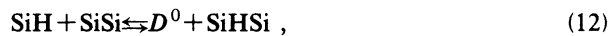


When the defects achieve equilibrium with the lattices, their concentration is given by the law of mass action:

$$[I] = [V] = ([V][I])^{1/2} \approx ([N_{\text{Si}}][N_{\text{Int}}])^{1/2} \times \exp(-E_I/2kT), \quad (11)$$

where E_I (~ 4 eV) is the energy required to form an interstitial-vacancy pair.¹

Neutral-defect formation in undoped *a*-Si:H can be described by a similar reaction:



where SiH are hydrogen atoms ($[\text{SiH}] \approx [\text{H}] \sim 0.1[\text{Si}]$) bonded to Si, whose motion enables the equilibration and SiHSi are H trapped at a weak-bond site, as illustrated in Fig. 2. In fact, several such reactions are possible and the temperature dependence of the defect concentration at equilibrium will strongly depend on the details of the reaction. A comparison between several possible defect reactions both with and without hydrogen has been made elsewhere.⁹

Reaction (12) produces equal numbers of two kinds of defects; spatially isolated dangling bonds (D^0) and intimate dangling-bond–bonded-hydrogen pairs (SiHSi). In principle, the different local environments of these two types of paramagnetic species should be distinguishable by hyperfine electron-spin resonance measurements. Such measurements find that greater than 50% of the dangling-bond charge is localized on the central Si atom with the remainder predominantly on at least one of the back-bonded neighbors.¹⁹ The tendency is for the remaining charge to be located on the back-bond away from the void into which the dangling bond “points.” This tendency, coupled with the estimated ~ 3 -Å effective microscopic localization radius of the dangling-bond wave function means that the hyperfine contact potential at the proton terminating the other half of the broken bond will be, in nearly all cases, exceedingly small. In practice, therefore, the two types of paramagnetic centers D^0 and SiHSi shown in Fig. 2(b) should be experimentally indistinguishable.

The application of the law of mass action to reaction (12) is similar to its application to reaction (5), except

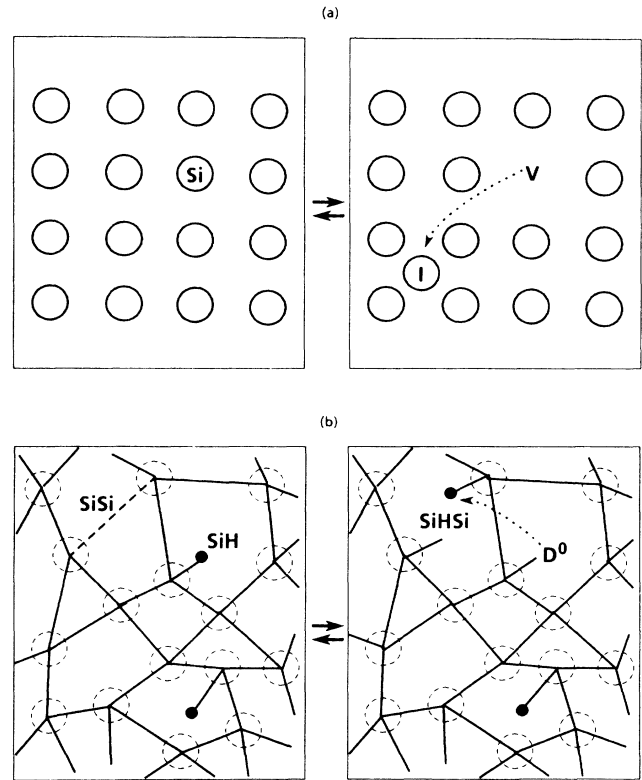


FIG. 2. Illustration of Frenkel defect formation in (a) crystalline silicon according to reaction (10) and (b) *a*-Si:H according to reaction (12).

now we take the defect-gap-state energy to be some arbitrary energy E^* as depicted in Fig. 3. The concentration of H atoms trapped at weak-bond sites whose states are in the interval between E and $E + dE$ is

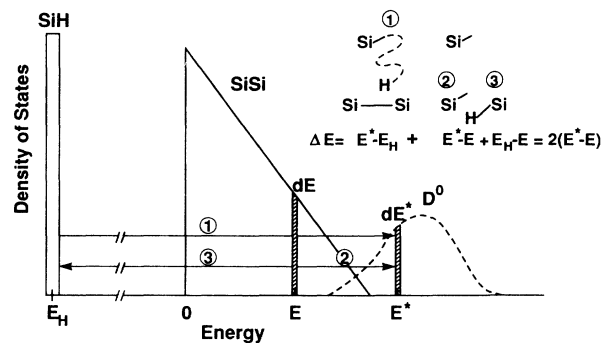


FIG. 3. Schematic density of states diagram, to illustrate the distribution of reaction enthalpies in the weak-bond–dangling-bond conversion model of Frenkel defect formation according to reaction (12). The distribution involves both an exponential component due to the exponential valence-band tail, and a Gaussian component due to the distribution of virtual defect states in the defect pool. The origin of the reaction enthalpy is illustrated in the inset.

$$\delta[\text{SiHSi}] = \frac{1}{2} \rho_{\text{SiHSi}}(E) dE = \frac{[H][\rho_{\text{SiSi}}(E) - \rho_{\text{SiHSi}}(E)] \exp(-\Delta E/kT)}{2[D^0]} dE, \quad (13)$$

where $\rho_{\text{SiSi}}(E)$ ($=2d[\text{SiSi}]/dE$) and $\rho_{\text{SiHSi}}(E)$ ($=2d[\text{SiHSi}]/dE$) are the density of weak SiSi bonding states in the absence of defects and the density of weak SiSi bonding states removed by hydrogen, respectively. $\Delta E = 2(E^* - E)$ is the formation enthalpy of a single SiHSi- D^0 pair (ionic and multielectronic effects are ignored) as described in Fig. 3. The resulting concentration of neutral-defect states between E^* and $E^* + dE^*$ for a δ -function defect distribution at equilibrium is

$$\begin{aligned} \frac{d[D^0]}{dE^*} &= 2 \sum_E \delta[\text{SiHSi}] \\ &= \int_0^\infty \frac{N_{v0} \exp(-E/E_0) dE}{1 + \frac{[D^0]}{[H]} \exp[2(E^* - E)/kT]} \delta(E^* - E_{D^0}). \end{aligned} \quad (14)$$

The integral expresses the defect density at $E^* = E_{D^0}$ as the total concentration of weak-bond states occupied (i.e., removed) by hydrogen, in analogy with Fermi occupation statistics, where the neutral-defect chemical potential $\mu_{D^0}(E^*) \equiv E^* + (kT/2) \ln([D^0]/[H])$ plays the role of the Fermi level. Equation (14) can be integrated to yield

$$[D^0] = \left[\frac{N_{v0} E_0 kT}{(2E_0 - kT)} \right] \left[\frac{2E_0}{kT} \exp[-\mu_{D^0}(E_{D^0})/E_0] - \exp[-2\mu_{D^0}(E_{D^0})/kT] \right]. \quad (15)$$

Equations (14) and (15) should be compared with Eq. (9). The numerical solution of Eq. (15) leads to a temperature dependence of $[D^0]$ ($-\partial \ln[D^0]/\partial(1/kT) \approx 0.2-0.3$ eV for $T \geq 500$ K) that agrees well with experiment.⁷⁻⁹ The reversible temperature dependence of $[D^0]$ is the main evidence for defect equilibration in *a*-Si:H and clearly demonstrates the essential role of entropy in this process, which strongly depends on the specific reaction considered.

The weak temperature dependence of Eq. (15) makes the $T=0$ limit, where $[D^0]$ reaches its minimum value a reasonably good approximation to $[D^0]$ at equilibrium.¹⁴ At $T=0$, Eq. (15) becomes

$$[D^0]|_{T=0} = N_{v0} E_0 \exp(-E_{D^0}/E_0). \quad (16)$$

The simplicity of this expression makes clear the important role of the valence-band-tail slope E_0 in determining the defect concentration in *a*-Si:H. The second important discovery by Smith and Wagner is that the defect concentration cannot be made arbitrarily small. No amount of deposition optimization can reduce the defect concentration in *a*-Si:H below the value set by Eq. (16). Only by reducing the slope of the valence-band tail can $[D^0]$ be reduced. The role of the growth conditions in determining

E_0 , and hence $[D^0]$, will be addressed in a later section.

It has been a long-standing problem in *a*-Si:H that with 10% hydrogen, the majority of which is known to occupy bond-terminating sites, there can still persist 10^{16} cm^{-3} unterminated dangling bonds. The problem is that any unterminated bonds should be immediately passivated by H, since H termination of dangling bonds is exothermic. However, at nonzero temperatures the entropy gained by defect formation will always ensure that some fraction of the SiH bonds are unoccupied by H (i.e., form defects). The reason why $[D^0]$ is not identically zero at $T=0$ is because there will always be some states in the exponential valence-band tail for which the defect-formation enthalpy $\Delta E = 2(E_{D^0} - E)$ will be negative (i.e., exothermic reaction). That is, all valence-band-tail states above and none below E_{D^0} will be occupied by H at equilibrium at $T=0$. However, it is unlikely that the $T=0$ equilibrium of Eq. (16) could ever be achieved because of the infinitesimally slow rate of equilibration in *a*-Si:H at this temperature.

D. Inclusion of the correlation and Fermi energies in the defect chemical potential

The addition of electrons from donor ionization in *n*-type *a*-Si:H changes the equilibrium point of reaction (12). Consider the additional reaction,



which, in the forward direction, describes the capture of an electron from the conduction band by a neutral defect. An increase in the number of electrons in the system pushes reaction (17) and, as a consequence, reaction (12) in the forward direction, which results in a larger deep-defect concentration. This process is independent of the origin of the extra electrons; defect creation by this process can result from applied fields, light exposure, doping, or activated gas adsorption, all of which can change the position of the electronic neutrality level. However, a shift in the Fermi energy to fill or empty defects states will not lead to a change in their distribution if the duration of the shift is much less than the characteristic equilibration time τ at a given temperature ($\tau \approx 10^6$ s at 300 K and ≈ 60 s at 400 K in *n*-type *a*-Si:H).^{4,6}

The increase in defect concentration comes about because the cost to form a defect is reduced by the energy gained in dropping an electron from the Fermi level onto the defect level (i.e., by $E_D - E_F$), while increased by the extra cost $U > 0$ of having two electrons occupy the same localized state (i.e., the electron-correlation energy). Thus, the concentration of charged defects in *n*-type *a*-Si:H at equilibrium is given by Eq. (15) with the neutral-defect chemical potential

$$\mu_{D^0}(E^*) \equiv E^* + (kT/2) \ln([D^0]/[H]) \quad (18)$$

replaced by the Fermi-energy-dependent chemical potential

$$\mu_{D^-} = 2E^* + U - E_F + (kT/2)\ln([D^-]/[H]). \quad (19)$$

Also, the defect energy E_{D^0} in the δ function in Eq. (14) must be replaced by $E_{D^0} + U$; the single D^- defect level must lie above the single D^0 defect level by an energy U . More generally, we could include the energy dependence of U in the formalism as has been attempted elsewhere.²⁰ The corresponding defect chemical potential for *p*-type *a*-Si:H is

$$\mu_{D^+} = E_F + (kT/2)\ln([D^+]/[H]). \quad (20)$$

The defect chemical potential (free energy per defect) plays a pivotal role in determining the equilibrium defect concentrations in *a*-Si:H, which is clear from Eq. (15). In addition, the defect chemical potential directly determines the distribution of defect states in the band gap through its dependence on the defect-state energy E^* . This is clearly demonstrated in Fig. 4, where Eqs. (18)–(20) are plotted as a function of E_F for three different values of E^* at $T=0$. For a given E_F , the concentration of the species with the lowest free energy will exponentially dominate at equilibrium. It is obvious from Fig. 4 that for a given E_F , the dominant species depends strongly on where in the gap the defect states lie.

E. The defect pool

The δ function in Eq. (14) represents the distribution of all possible (“virtual”) defect-state energies at which the system can choose to create defect states in order to minimize the system free energy. In this particular case, the equilibrium defect distribution and the distribution of virtual states are identical, and the system free-energy

$$\frac{d[D^0]}{dE^*} = \left[\frac{N_{v0}E_0kT}{(2E_0 - kT)} \right] \left[\frac{2E_0}{kT} \exp[-\mu_{D^0}(E^*)/E_0] - \exp[-2\mu_{D^0}(E^*)/kT] \right] \frac{\exp[-(E^* - E_p)^2/2\sigma^2]}{(2\pi\sigma^2)^{1/2}}, \quad (21)$$

where the integral in Eq. (14) has been explicitly evaluated with the restriction that $\mu_{D^0}(E^*) \geq 0$, σ is the standard deviation of the Gaussian defect-pool distribution, and E_p is the energy of the most probable defect configuration, i.e., the defect-pool maximum. A candidate for the physical manifestation of the defect pool, according to reaction (12), is the large concentration of bonded hydrogen, where the variable backbond strain gives rise to the broad distribution of potential defect sites. Thus, σ should be a characteristic measure of disorder in *a*-Si:H as has been proposed for E_0 , both of which might be described by a single-disorder parameter such as the average bond-angle deviation.

The maximum of the defect distribution can be calculated by extremizing Eq. (21) with respect to E^* , which for $kT/2 < E_0$ gives $E_{D^0} \equiv E_{\max}^* = E_p - \sigma^2/E_0$. This is just what is required to cancel the first (second when

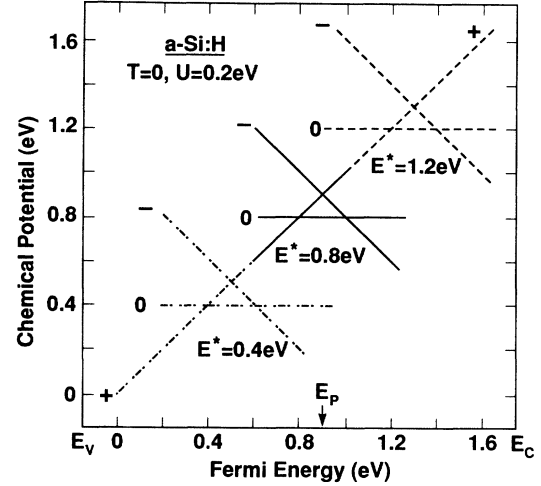


FIG. 4. Chemical potential (free energy per defect) for neutral (0), positively (+), and negatively (-) charged defects in *a*-Si:H at $T=0$ according to Eqs. (18–20) as a function of E_F for defect states located at $E^* - E_v = 0.4, 0.8,$ and 1.2 eV. The proportion of neutral and charged defects for a given Fermi energy strongly depends on where in the gap the defects states lie. Note that the D^- chemical potential can become negative for $E^* < 0.8$ eV.

minimum is determined by a balance between the entropy produced via defect creation and the enthalpy cost of transferring H from bond-terminating sites to weak-bond trapping sites. However, if we replace the δ function in Eq. (14) with a more general Gaussian distribution of virtual defect energies (i.e., a “defect pool”), the system free energy can be further reduced through a lowering of the transfer enthalpy.²¹ The defect density becomes

$kT/2 > E_0$) exponential in Eq. (21), which results in an observed defect distribution $d[D^0]/dE^*$ that is Gaussian with width σ and a peak at $E_p - \sigma^2/E_0$ ($E_p - 2\sigma^2/kT$ when $kT/2 > E_0$). The shift is due to the balance between a defect-formation energy reduction [$\propto (E^* - E_p)$] for defect states formed in the low-energy tail of the defect-pool distribution and an addition [$\propto (E^* - E_p)^2$] due to the increased distortion energy for states formed far from the defect-pool maximum, which results in a system free-energy change $\Delta G \approx -\sigma^2/E_0$. The distribution of defect energies (“defect-pool”) results in the creation of the majority of neutral defects not at an energy where potential defect sites are least distorted due to background strain and most numerous (i.e., at E_p), but where it costs the system the least free energy (i.e., at $E_p - \sigma^2/E_0$). A similar result has been suggested on the basis of more qualitative arguments.^{15,22–24} Note that, with a broad

defect-pool distribution, the two defects produced by reaction (12) need not have the same defect-state energy. The modification of Eq. (21) to take this into account is straightforward and results in a single Gaussian defect band peaked at $E_p - \sigma^2/2E_0$. In the following, we ignore this distinction and assume both defects have the same energy for simplicity.

Using the defect chemical potential for D^- defects Eq. (19), it is easy to show that the maximum of the resulting defect distribution in n -type a -Si:H at equilibrium occurs at $E_{D^-} \equiv E_{\max}^* = E_p + U - 2\sigma^2/E_0$. At equilibrium, D^0 in intrinsic a -Si:H is separated from D^- in n -type a -Si:H by an amount $\Delta E^{-/0} \equiv E_{D^-} - E_{D^0} = U - \sigma^2/E_0$. In the limit that $\sigma \rightarrow 0$ we recover the result $\Delta E^{-/0} = U$ expected for a single-correlated defect level. It can be similarly shown that $E_{D^+} = E_p$, and the shift between D^- in n -type and D^+ in p -type a -Si:H at equilibrium is given by $\Delta E^{-/+} \equiv E_{D^-} - E_{D^+} = U - 2\sigma^2/E_0$. The resulting shifts have a plausible physical origin, which is captured by the phenomenological model. The one electron occupying D^0 states can interact with the neighboring backbonds. The disorder of the backbonds is characterized by σ , and is the origin of the average σ^2/E_0 shifts in D^0 state energies. This shift is doubled for D^- states because they are occupied by two electrons. Correspondingly, the unoccupied D^+ states are not affected by the disorder. This could easily be tested by direct calculation.

IV. RESULTS AND DISCUSSION

We now put together all of the elements of the theory to calculate the equilibrium defect-state distributions and defect concentrations in a -Si:H as a function of temperature and Fermi energy. We employ Eq. (21) for the calculations and adopt the following experimentally deter-

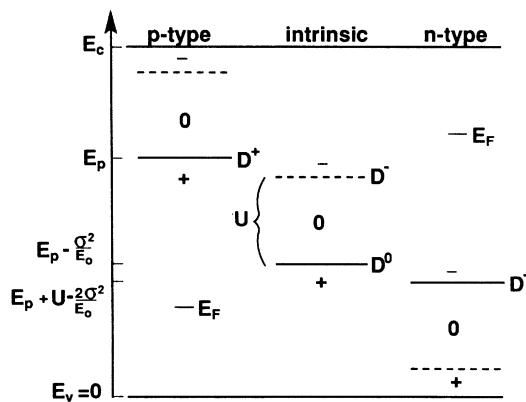


FIG. 5. Schematic ordering of defect transition energies in a -Si:H; +, 0, and - refer to the charge state of the majority of the defects when the Fermi energy is momentarily shifted below, in between, or above the two correlated levels, respectively. The 0/+ transition corresponds to the D^+ defect-band peak in p type and the D^0 defect-band peak in undoped, and the -/0 transition to the D^- defect-band peak in n -type a -Si:H at equilibrium.

mined values for the parameters of the theory:^{22,25-28} $N_{v0} = 2 \times 10^{20} \text{ eV}^{-1} \text{ cm}^{-3}$, $[H] = 5 \times 10^{21} \text{ cm}^{-3}$, $E_0 = 0.045 \text{ eV}$, $U = 0.2 \text{ eV}$, $\sigma = 0.125 \text{ eV}$, $E_{v0} \equiv 0.0 \text{ eV}$, $E_c - E_{v0} = 1.75 \text{ eV}$, and $E_{\text{gap}} = 1.9 \text{ eV}$. In addition, the peak of the defect-pool distribution ($E_p = 0.9 \text{ eV}$) is chosen such that $E_{D^0} = E_c - 1.2 \text{ eV}$. Improvements in the accuracy of all of these parameters are desirable, but they are sufficiently accurate to allow a test of the validity of the theory. However, Eq. (21) is only valid when the defect chemical potential μ is positive. In n -type material, μ is negative over a small energy range (see Fig. 4). In this case, E_{v0} was extended to -0.7 to compensate, which corresponds to an unphysically extended exponential tail. While this difficulty can be removed by reducing σ and U in such a manner as to retain the correct relative defect-state energy shifts, the n -type calculations were all performed with the above parameters and the valence-band-tail extension for consistency.

A. Distribution of defect states in a -Si:H

Using the above parameters, the theory predicts shifts $\Delta E^{-/0} \sim -0.15 \text{ eV}$ and $\Delta E^{-/+} \sim -0.50 \text{ eV}$, which are in reasonable agreement with the results of recent photoemission ($\Delta E^{-/0} = -0.15 \text{ eV}$ and $\Delta E^{-/+} \approx -0.7 \text{ eV}$) (Ref. 22) and optical-absorption ($\Delta E^{-/0} = -0.1 \text{ eV}$ and $\Delta E^{-/+} = -0.5 \text{ eV}$) (Refs. 26 and 27) measurements. The resulting ordering of 0/+ and -/0 defect transition energies for p -type, intrinsic, and n -type a -Si:H is shown schematically in Fig. 5. The resulting equilibrium defect

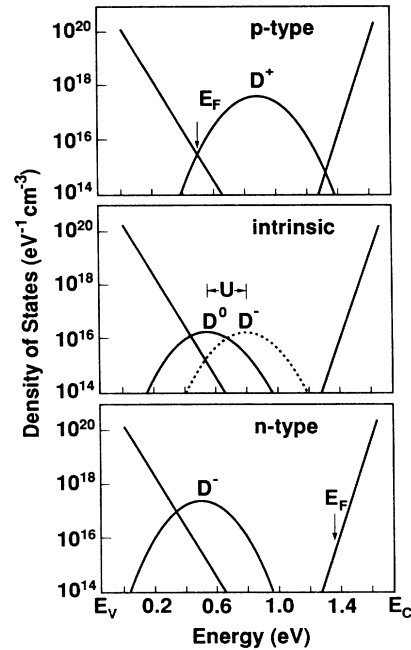


FIG. 6. Gap-state defect distributions for n -type, intrinsic, and p -type a -Si:H calculated using Eq. (21) with the appropriate defect chemical potentials and the parameters given in the text, except that $U = 0.25 \text{ eV}$.

distributions calculated from Eq. (21) are shown in Fig. 6 and compare well with the experimentally determined distributions.^{22,26,27} The important point is that for a wide enough defect-pool distribution ($\sigma > 0.1$ eV), D^- in *n*-type *a*-Si:H can lie deeper than D^0 in undoped *a*-Si:H at equilibrium even though the correlation energy is positive. This resolves the apparent experimental contradiction between electron-spin resonance data,^{29,30} which require a positive correlation energy, and equilibrium gap-state spectra,^{22,26,27} which show D^- in *n*-type *a*-Si:H to lie deeper than D^0 in undoped *a*-Si:H as might be expected for negative- U defects with fixed defect energies. A similar result has been obtained by Branz and Silver³¹ based on the idea of disorder-induced potential fluctuations that modify the reaction enthalpies and lead to shifts in the defect transition energies. The two approaches are similar, but the predicted defect concentrations as a function of Fermi energy are quite different.

B. Dependence of *a*-Si:H defect concentrations on Fermi energy and temperature

The equilibrium defect concentration as a function of Fermi energy for *a*-Si:H at 500 K is shown in Fig. 7. This is a reasonable freeze-in temperature with which to compare the results of the theory to experimental data. The neutral-defect concentration calculated for intrinsic *a*-Si:H agrees well with the lowest spin concentrations measured by electron-spin resonance (ESR).³² The calculated equilibrium-charged defect concentrations ($[D^-]$, $[D^+]$) increase exponentially with increasing separation of the Fermi energy from midgap with a slope

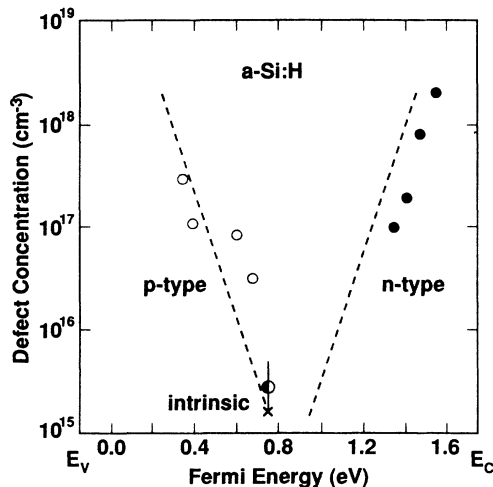


FIG. 7. Calculated equilibrium defect concentration in *a*-Si:H as a function of Fermi energy at 500 K from Eq. (21), with the parameters given in the text (dashed lines and cross). Data from photothermal deflection spectroscopy (Ref. 32) and conductivity activation energies (Ref. 34) P-doped (solid circles), B-doped (open circles), and undoped (half-filled circle) *a*-Si:H are shown for comparison.

$kT_0 \equiv E_0 + kT/2 = 67$ meV for both *n*- and *p*-type *a*-Si:H. This also agrees reasonably well with the data from photothermal deflection spectroscopy (PDS)^{32,33} and conductivity activation energy measurements,³⁴ which for P-doped *a*-Si:H $kT_0 \approx 59$ meV.

Although we have assumed that the intrinsic Fermi energy ($E_I = 0.75$ eV) lies at the intersection point of the *p*-type and intrinsic curves, the charged defect concentrations in *a*-Si:H are quite small when E_F is near midgap, in agreement with experiment. However, this is different from the results of the potential fluctuation theory of Branz and Silver,³¹ which predicts large concentrations of both D^- and D^+ states in undoped (intrinsic) *a*-Si:H at equilibrium. Their model postulates a heterogeneous *a*-Si:H structure containing potential fluctuations over many nanometers. These fluctuations effectively shift the local-reaction enthalpies by the amount of the local potential. In doped *a*-Si:H, moderate potential shifts do not perturb the dominant enthalpy shift due to the Fermi energy movement toward either band edge, which maintains large concentrations of either D^- or D^+ as in Fig. 7. However, in undoped *a*-Si:H, although the average enthalpy shift is zero, moderate potential fluctuations lead to large concentrations of spatially separated D^- and D^+ states according to the sign of the local potential fluctuation. More detailed measurements of the total defect concentration as a function of Fermi energy are

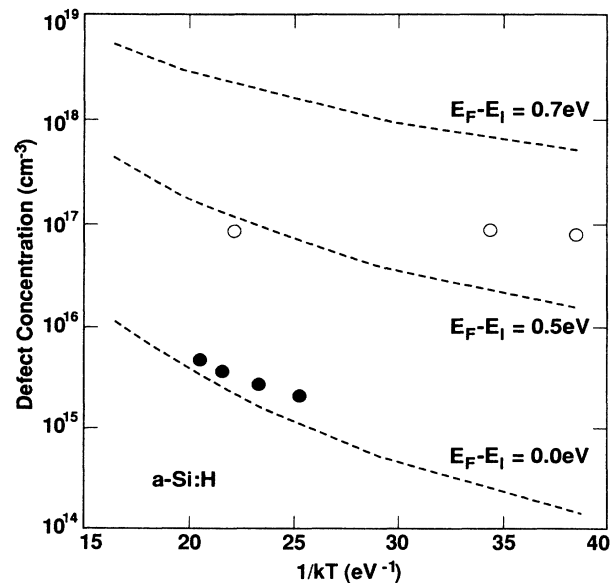


FIG. 8. Calculated equilibrium defect concentrations in *a*-Si:H as a function of inverse temperature for different Fermi energies from Eq. (21) with the parameters given in the text (dashed lines). $E_F - E_I = 0.0, 0.5,$ and 0.7 eV corresponds to undoped, 10^{-5} P-doped, and 10^{-2} P-doped *a*-Si:H, respectively. Data from undoped *a*-Si:H by electron-spin resonance (solid circles) and 10^{-5} P-doped *a*-Si:H by photothermal deflection spectroscopy (open circles) are shown for comparison (Refs. 9 and 18).

needed to completely resolve this issue, but the data so far available do not support this prediction of the potential fluctuation theory.^{32,33}

The temperature dependence of the equilibrium defect concentration as a function of Fermi energy is shown in Fig. 8. In intrinsic *a*-Si:H, the high-temperature slope of the calculated curve is ≈ 0.3 eV. This decreases to ≈ 0.23 eV for $E_F - E_I = 0.5$ eV (equivalent to 10^{-5} P-doped *a*-Si:H) and to ≈ 0.15 eV for $E_F - E_I = 0.7$ eV (equivalent to 10^{-2} P-doped *a*-Si:H). The neutral-defect concentration in undoped *a*-Si:H determined by ESR measurements agrees with the intrinsic calculation.⁹ However, little change in the D^- defect concentration is detected by photothermal deflection spectroscopy for 10^{-5} P-doped *a*-Si:H contrary to the calculation,¹⁸ although the general trend toward less temperature sensitivity with increased doping is correct. The maximum defect concentration permitted by this theory is $N_{v0}E_0 = 9 \times 10^{18} \text{ cm}^{-3}$, which corresponds to the $T \rightarrow \infty$ limit, where all weak-bond states are broken and converted into defects. It is clear that as the 500-K equilibrium concentration becomes larger with increased $E_F - E_I$, the weaker should become the temperature dependence of $[D^-]$. However, the temperature dependence of the active dopant concentration and, hence, E_F has not been taken into account here, which might account for the weaker than predicted temperature dependence.

C. Defect formation in other hydrogenated amorphous semiconductors: *a*-Ge:H

The properties of other hydrogenated amorphous semiconductors can be described in terms of this defect-

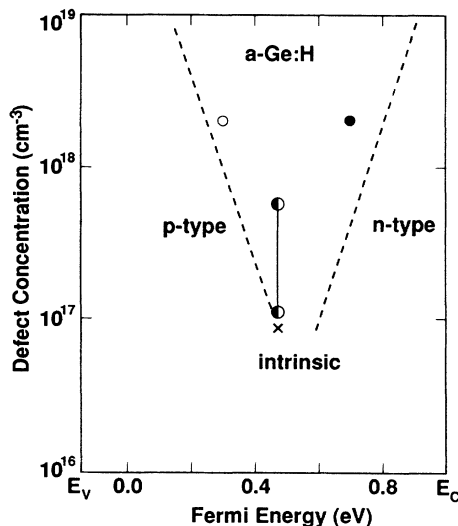


FIG. 9. Calculated equilibrium defect concentration in *a*-Ge:H as a function of Fermi energy at 500 K from Eq. (21) with the parameters given in the text (dashed lines and cross). Data from photothermal deflection spectroscopy and conductivity activation energies for P-doped (solid circle), B-doped (open circle), and undoped (half-filled circles) *a*-Ge:H are shown for comparison (Refs. 32 and 35).

formation theory. As an example, the calculated equilibrium defect concentration of *a*-Ge:H at 500 K as a function of Fermi energy is shown in Fig. 9. *a*-Ge:H has an optical gap of 1.15 eV compared to that of *a*-Si:H of 1.9 eV. The peak of the defect-pool distribution has been decreased from 0.9 eV to $0.9 \times 1.15/1.9 = 0.54$ eV accordingly. Also, the full width at half maximum of the defect pool has been decreased from 0.3 eV ($\sigma = 0.125$ eV) to 0.2 eV ($\sigma = 0.085$ eV) in agreement with recent experimental data.³⁵ Again the equilibrium defect concentrations increase exponentially as the separation between the Fermi energy and midgap increases with a slope of $E_0 + kT/2$. The little available data are consistent with the calculations,^{32,35} except that the measured neutral-defect concentration is observed to lie well above the calculated equilibrium value in some instances.³² Such variations are well known to result from material growth far from the optimal deposition conditions.

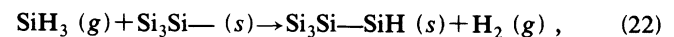
V. OPTIMAL GROWTH

The success of the chemical approach to understanding the behavior of defects in *a*-Si:H can also be carried over into the description of optimal growth of *a*-Si:H, defined here as those growth conditions that lead to the lowest equilibrium defect concentration. The key idea for this approach is that the main role of the plasma is to supply the sources of chemically reactive species, but the *a*-Si:H material properties are determined for the most part by chemical reactions that take place on or below the growth surface. The reliance on solid-state chemical reactions rather than plasma-gas processes is radically different from most previous attempts to describe *a*-Si:H growth. Such attempts have emphasized plasma reactions and the kinematics of surface accretion. However, the fact that *a*-Si:H films produced in remote hydrogen plasma reactors, where uv light exposure and charged particle bombardment are absent, are indistinguishable from those produced in rf glow discharge reactors³⁶ suggests that plasma-related effects are not crucial in determining *a*-Si:H material properties.

A. Quasiequilibrium growth model

We consider only undoped *a*-Si:H growth from silane (SiH_4) and treat *a*-Si:H as a homogeneous ensemble of Si—Si and Si—H bonds. The defect concentration $[D^0]$ serves as the measure of material quality. The growth model consists of the following reactions.

Si-Si and Si-H incorporation. SiH_3 has been demonstrated to be one important gaseous precursor for *a*-Si:H growth.³⁷ Therefore, Si-H and Si-Si incorporation during growth may be described stoichiometrically by the following reaction:³⁸



where $\text{Si}_3\text{Si}-(s)$ is a surface dangling bond (D^0), (g) and (s) refer to gas- and solid-phase species, and the subscripts refer to the number of atoms in the species (i.e., $\text{Si}_3\text{Si}-\text{SiH}$ is a Si atom bonded to three Si atoms and one SiH unit). This reaction proceeds at a rate proportional

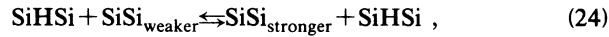
to the plasma power P .

Neutral-defect formation. Defect formation occurs as already described:



Both the forward and reverse rates depend on the rate of dispersive hydrogen diffusion and, therefore, on the substrate temperature T_s . At equilibrium, $[D^0]$ is a simple function of the temperature T and valence-band-tail slope E_0 [Eq. (21)]; the greater E_0 is, the greater is $[D^0]$.

Strain reduction. A mechanism of strain reduction is required for equilibration of the film to proceed. This can be accomplished by the following reaction:³⁹



which is exothermic in the forward direction. The forward reaction proceeds until the valence-band tail is sufficiently narrowed to reach equilibrium if there is sufficient time to do so near the surface during growth. Below the surface, bulk constraints increase the kinetic barrier(s) of the reaction. The equilibration rate depends on the rate of H diffusion and, therefore, on T_s . Both reactions (23) and (24) (at least in the forward direction for the latter) can proceed after deposition; in this case, their rates depend on T . When reaction (24) can reach equilibrium during growth, the concentration of weak SiSi bonds between an energy E and $E + dE$ should be approximately given by

$$[\text{SiSi}] \approx N_{v0} \exp(-E/kT_s) dE \quad (25)$$

where $E - E_{v0}$ is the weak-bond-formation enthalpy and $kT_s = E_0$ is the valence-band-tail slope. In this case, the greater T_s is, the greater should be E_0 and, therefore, $[D^0]$.

Reaction (22) describes transport of SiSi and SiH bonds into the growing film. Reactions (23) and (24) describe bulk chemical reactions between these species whose kinetics depend only on temperature. The material properties of *a*-Si:H depend on the relative rates of these three reactions, which are determined by two growth parameters: P and T_s . We now apply this model to interpret the conditions of optimal *a*-Si:H growth.

B. Optimal *a*-Si:H growth and irreversible defect annealing

In undoped *a*-Si:H films grown under the empirically determined "optimal" conditions of $P \sim 2$ W and $T_s \sim 230$ °C, $[D^0]$ and E_0 attain their minimum values of $\sim 10^{16} \text{ cm}^{-3}$ and 45 meV, respectively.⁴⁰ Post-deposition thermal annealing of optimally grown *a*-Si:H at, say, 300 °C leads to the reversible increase of $[D^0]$ according to Eq. (21) as the equilibrium point of reaction (23) is momentarily pushed in the forward direction,⁷⁻⁹ while E_0 is essentially unchanged.^{18,41} When conditions deviate from the optimal and *a*-Si:H is grown at low temperature and high plasma power, $[D^0]$ and E_0 are much larger (up to 10^{18} cm^{-3} and 100 meV, respectively) and sufficient post-deposition annealing at 300 °C can lead to

the irreversible decrease of both $[D^0]$ and E_0 to near their optimal values without H loss.^{42,43}

The effect of plasma power P and substrate temperature T_s on $[D^0]$ and E_0 can be cast in terms of a competition between the rate of H diffusion in the film, which controls the rates of reactions (23) and (24) and increases with T_s , and the rate of film growth R , which increases with P . Because the dependence of $[D^0]$ on E_0 is found to hold even in films grown far from optimal conditions,^{9,43} reaction (24) is most likely the rate limiting step for optimal *a*-Si:H growth. If R is high or T_s low, then H diffusion will not be able to equilibrate the near surface fast enough to keep up with the deposition rate. Inhomogeneous equilibration will result. Upon thermal annealing after deposition, reaction (24) will continue in the forward direction and the equilibrium point of reaction (23) will shift accordingly (i.e., $[D^0]$ will decrease as E_0 decreases). A similar optimal growth model that relates material quality to the surface diffusion length of SiH₃ precursors has been proposed by Tanaka and Matsuda.⁴⁴ Although the physical details of their model are different, it and the present model share an important feature. That material quality is determined by some process other than the simple defect reaction of Eq. (23) that is kinetically limited by near surface diffusion and, therefore, highly dependent on the growth rate.

In order for optimal growth to occur, the average rate of H diffusion v_H in the time interval Δt should be roughly equal to the growth rate R ,

$$v_H \equiv (4D_H/\Delta t)^{1/2} \approx R \approx 4D_H/L \quad (26)$$

where D_H is the H diffusion constant in *a*-Si:H (Ref. 45) and $L \equiv R \Delta t$, such that the time available for equilibration in the less constrained near-surface layer of thickness L decreases as R increases. Agreement with the data is obtained with $L = 1$ Å, which suggests a surface-limited equilibrium growth process. Of course, Eq. (26) is approximate, and does not take into account the dispersive nature of H diffusion.⁴⁵ Under condition (26), which we take as the definition of optimal *a*-Si:H growth, reactions (23) and (24) can achieve equilibrium during deposition. This definition is quantified in Fig. 10, where the *a*-Si:H growth rate is plotted as a function of rf plasma power P and compared to v_H ($L = 1$ Å) at various T_s . For a given P , the optimal T_s should be approximately given by the temperature at which v_H equals R . Thus at $P = 2$ W, R is ≈ 1 Å/s and the temperature at which v_H equals R is ≈ 250 °C. This is the growth temperature at which $[D^0]$ and E_0 are minimum for $P = 2$ W.⁴⁰ At higher P , a higher T_s should be required to achieve optimal growth.

The dependence of $[D^0]$ on growth temperature T_s should follow a "U"-shaped curve whose minimum corresponds to the optimal T_s . The low-temperature part of the curve corresponds to the premature arrest of reaction (24), while the high-temperature part results from the increased valence-band-tail slope $E_0 = kT_s$. When T_s is low, reaction (24) cannot proceed appreciably and a large density of weak bonds is built into the amorphous network. Although post-deposition annealing above the low T_s will remove the weakest bonds via reaction (24), bulk

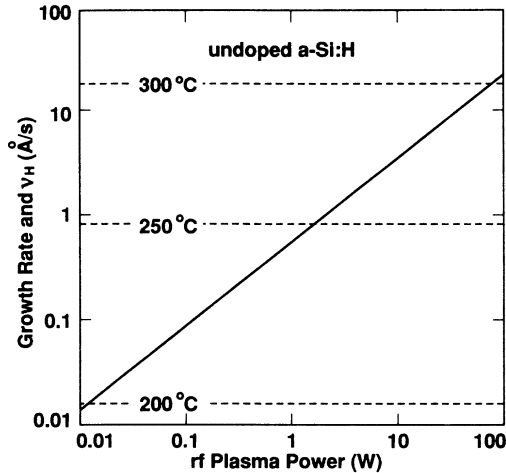


FIG. 10. *a*-Si:H growth rate vs rf plasma power (solid line). Also plotted are the H diffusion rates v_H from Eq. (26) (dashed lines), whose intersection with the growth rate curve denotes the optimal growth condition.

constraints will prevent the achievement of material properties as good as those in films grown under optimal conditions. When T_s is high, reactions (23) and (24) can achieve equilibrium at and below the growth surface. At equilibrium, $[SiSi]$ and $[D^0]$ will be determined by T_s and higher values than the optimal can be “frozen” into the film during growth. The optimal growth temperature should be reduced under hydrogen dilution due to the reduced growth rates.

The optimal growth temperature T_s should, in general, increase with rf power P and decrease with H_2 dilution. Electron-spin-resonance (ESR) measurements of the spin (neutral-defect) concentration of undoped *a*-Si:H grown with no H_2 dilution as a function of T_s partially support this expectation (Fig. 11). The optimal T_s for pure silane growth increases from $\approx 250^\circ C$ at $P=2$ W to $> 300^\circ C$ at $P=60$ W, which is in reasonable agreement with Eq. (26) and Fig. 10. Also, a reduction in optimal growth temperature at reduced *a*-Si:H growth rates has been observed in remote plasma reactors.⁴⁶ Although this T_s dependence is relatively weak, it is clear from the data so far available that solid-state chemical equilibrium models of optimal *a*-Si:H growth are worthy of further consideration.

VI. SUMMARY AND CONCLUSIONS

The elements of a quantitative theory of defect formation in *a*-Si:H based on the thermodynamic analysis of simple chemical reactions were described and employed to calculate the defect distributions and concentrations as a function of Fermi energy and temperature. The results

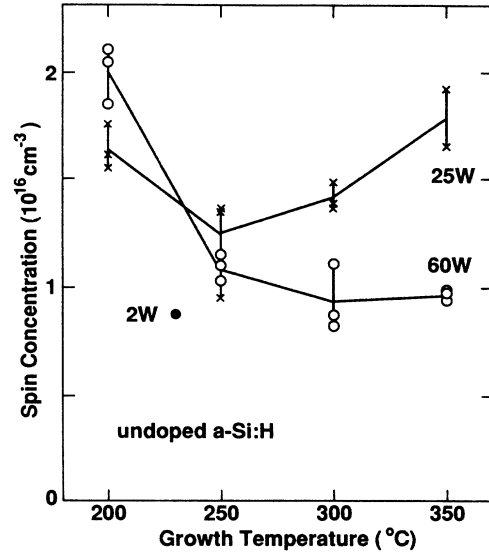


FIG. 11. Spin (neutral defect) concentration of undoped *a*-Si:H measured by ESR as a function of growth temperature with no H_2 dilution, which shows the increase in the optimal growth temperature with increasing rf power expected from the growth model.

compared favorably with the available experimental data suggesting that the underlying basis of the theory is essentially correct. The applicability of the theory to other hydrogenated amorphous semiconductors was also demonstrated. Optimal growth of *a*-Si:H was considered within a similar chemical framework and the optimal growth temperature for undoped *a*-Si:H deposition was predicted to weakly depend on growth rate. Preliminary data was presented to support this prediction.

The great advantage of a chemical equilibrium framework within which to describe defect formation in *a*-Si:H lies in the simple, intuitive, and analytical expressions that result for the concentration and distribution of defect states in the band gap. There is every reason to believe that the theory can be extended to other hydrogenated amorphous semiconductors with similar success. The challenge for future work is to discover from this intuitive picture of band-tail and defect-state equilibrium how to better control the material properties of *a*-Si:H.

ACKNOWLEDGMENTS

I thank Bob Street, Warren Jackson, Z Smith, Sigurd Wagner, Martin Stutzmann, Howard Branz, and Marvin Silver for many useful discussions. Work supported by the Solar Energy Research Institute (Golden, CO).

*Present address: NTT Basic Research Laboratories, Nippon Telegraph and Telephone Corporation, 3-9-11 Midori-cho, Musashino-shi, Tokyo 180, Japan.

¹N. B. Hannay, *Solid-State Chemistry* (Prentice-Hall, Engle-

wood Cliffs, NJ, 1967).

²R. A. Street, J. Kakalios, and T. M. Hayes, *Phys. Rev. B* **34**, 303 (1986).

³Z. Smith, S. Aljishi, D. Slobodin, V. Chu, S. Wagner, P. M.

- Lenahan, R. R. Arya, and M. S. Bennett, *Phys. Rev. Lett.* **57**, 2450 (1986).
- ⁴K. Winer and W. B. Jackson, *Phys. Rev. B* **40**, 12558 (1989).
- ⁵W. J. Moore, *Physical Chemistry* (Prentice-Hall, Englewood Cliffs, NJ, 1959).
- ⁶W. B. Jackson, *Phys. Rev. B* **41**, 1059 (1990).
- ⁷X. Xu, A. Okumura, A. Morimoto, M. Kumeda, and T. Shimizu, *Phys. Rev. B* **38**, 8371 (1988).
- ⁸S. Zafar and E. A. Schiff, *Phys. Rev. B* **40**, 5235 (1989).
- ⁹R. A. Street and K. Winer, *Phys. Rev. B* **40**, 6236 (1989).
- ¹⁰Z. Smith and S. Wagner, *Phys. Rev. Lett.* **59**, 688 (1987).
- ¹¹M. Stutzmann, *Philos. Mag. B* **56**, 63 (1987).
- ¹²V. Heine, in *Solid State Physics*, edited by H. Ehrenreich, F. Seitz, and D. Turnbull (Academic, New York, 1980), Chap. 1, p. 188.
- ¹³W. B. Jackson and N. M. Amer, *J. Phys. Colloq.* **42**, C4-293 (1981).
- ¹⁴M. Stutzmann, *Philos. Mag. B* **60**, 531 (1989).
- ¹⁵Z. Smith and S. Wagner, in *Amorphous Silicon and Related Materials*, edited by H. Fritzsche (World Scientific, Singapore, 1988), p. 409.
- ¹⁶R. A. Street, J. Kakalios, C. C. Tsai, and T. M. Hayes, *Phys. Rev. B* **35**, 1316 (1987).
- ¹⁷J. Kakalios, R. A. Street, and W. B. Jackson, *Phys. Rev. Lett.* **59**, 1037 (1987).
- ¹⁸R. A. Street, M. Hack, and W. B. Jackson, *Phys. Rev. B* **37**, 4209 (1988).
- ¹⁹D. K. Biegelsen and M. Stutzmann, *Phys. Rev. B* **33**, 3006 (1986).
- ²⁰L. Schweitzer, M. Grunewald, and H. Dersch, *J. Phys. (Paris) Colloq.* **42**, C4-827 (1981).
- ²¹K. Winer, *Phys. Rev. Lett.* **63**, 1487 (1989). The term *defect pool* was first used by L. Ley to describe the observed Fermi-energy-dependent shifts in the defect levels in *a*-Si:H.
- ²²K. Winer, I. Hirabayashi, and L. Ley, *Phys. Rev. Lett.* **60**, 2697 (1988); *Phys. Rev. B* **38**, 7680 (1988).
- ²³Y. Bar-Yam, D. Adler, and J. D. Joannopoulos, *Phys. Rev. Lett.* **57**, 467 (1986).
- ²⁴K. Winer and L. Ley, in *Amorphous Silicon and Related Materials*, edited by H. Fritzsche (World Scientific, Singapore, 1988), p. 365; L. Ley and K. Winer, in *Proceedings of the 19th International Conference on the Physics of Semiconductors*, edited by W. Zawadzki (PIOP, Warsaw, 1989), p. 1633.
- ²⁵N. M. Johnson and D. K. Biegelsen, *Phys. Rev. B* **31**, 4066 (1985).
- ²⁶J. Kocka, M. Vanacek, and A. Triska, in *Amorphous Silicon and Related Materials*, edited by H. Fritzsche (World Scientific, Singapore, 1988), p. 297.
- ²⁷K. Pierz, W. Fuhs, and H. Mell, *J. Non-Cryst. Solids* (to be published).
- ²⁸W. B. Jackson, *Solid State Commun.* **44**, 477 (1982).
- ²⁹R. A. Street and D. K. Biegelsen, *Solid State Commun.* **33**, 1159 (1980).
- ³⁰H. Dersch, J. Stuke, and J. Beichler, *Phys. Status Solidi B* **105**, 265 (1981).
- ³¹H. M. Branz and M. Silver (unpublished).
- ³²M. Stutzmann, D. K. Biegelsen, and R. A. Street, *Phys. Rev. B* **35** (1987).
- ³³K. Pierz, W. Fuhs, H. Mell, *J. Non-Cryst. Solids* **114**, 651 (1989).
- ³⁴J. Kakalios and R. A. Street, *Phys. Rev. B* **34**, 6014 (1986).
- ³⁵S. Aljishi, Jin Shu, and L. Ley, *Mater. Res. Soc. Symp. Proc.* **149**, 125 (1989).
- ³⁶N. M. Johnson, J. Walker, C. M. Doland, K. Winer, and R. A. Street, *Appl. Phys. Lett.* **54**, 1872 (1989).
- ³⁷R. Robertson, D. Hills, H. Chatham, and A. Gallagher, *Appl. Phys. Lett.* **43**, 544 (1983).
- ³⁸More detailed surface accumulation reactions are discussed by A. Gallagher, *J. Appl. Phys.* **63**, 2406 (1988).
- ³⁹K. Winer, *Appl. Phys. Lett.* **55**, 1759 (1989).
- ⁴⁰*Hydrogenated Amorphous Silicon*, edited by J. I. Pankove, Vol. a of *Semiconductors and Semimetals* (Academic, New York, 1984).
- ⁴¹S. Aljishi, J. D. Cohen, and L. Ley, *J. Non-Cryst. Solids* **114**, 247 (1989).
- ⁴²D. K. Biegelsen, R. A. Street, C. C. Tsai, and J. C. Knights, *Phys. Rev. B* **20**, 4839 (1979).
- ⁴³R. A. Street and K. Winer, *Mater. Res. Soc. Symp. Proc.* **149**, 131 (1989).
- ⁴⁴K. Tanaka and A. Matsuda, *Mater. Sci. Rep.* **3**, 142 (1987).
- ⁴⁵R. A. Street, C. C. Tsai, J. Kakalios, and W. B. Jackson, *Philos. Mag.* **56**, 305 (1987).
- ⁴⁶G. N. Parsons, D. V. Tsu, and G. Lucovsky, *Mater. Res. Soc. Symp. Proc.* **118**, 37 (1988).